Clay Minerals, (2010) **45**, 229–240

Mineralogical and physicochemical characterization of selected Portuguese Mesozoic-Cenozoic muddy/clayey raw materials to be potentially used as healing clays

M. REBELO*, F. ROCHA AND E. FERREIRA DA SILVA

GEOBIOTEC, Geoscience Department, University of Aveiro, Campus Universitário de Santiago, 3810-193 Aveiro, Portugal

(*Received 21 December 2007; revised 10 February 2010; Editor: George Christidis*)

ABSTRACT: The use of pelitic geological materials for the treatment of muscle-bone-skin pathologies, by application of a cataplasm made of clay and mineral water mixture, is currently receiving attention and interest from the general public and scientific community. In Portugal there are several natural occurrences of clays/muds which are used for pelotherapy and/or geotherapy. These are carried out either indoors (thalassotherapy and thermal centres) or outdoors, in natural sites generally located near the seaside. The aim of this study is to assess the mineralogical and physicochemical properties of Portuguese raw materials for therapeutic purposes. These materials were collected from different Portuguese Mesozoic-Cenozoic geological formations located in the neighbourhood of thermal centres or at beaches known from their empirical applications. X-ray diffraction (XRD) and scanning electron microscopy (SEM-EDS) were used to assess the mineralogical composition of these clays. Physicochemical properties, such as specific surface area, cation exchange capacity, plasticity/abrasiveness indices and heat diffusiveness were also determined. Having distinct geological ages and genesis, the materials examined are mainly illitic. Less abundant kaolinite and smectite are also present. With respect to their physicochemical properties, all samples have good thermal properties which make them potentially suitable for therapeutic or aesthetic purposes.

KEYWORDS: clay minerals, physicochemical properties, thermal mud, medicinal use, geotherapy, pelotherapy, muddy/clayey raw materials, Portugal.

Clay minerals have been used for medicinal purposes since ancient times, although the first uses were based on empirical applications[1]. The growing interest in human health and welfare has increased the study of clay minerals for therapeutic and aesthetic purposes.

Clay minerals are commonly used for the preparation of thermal muds, applied in geotherapy or pelotherapy (Carretero, 2002). These applications are carried out in thermal centres for the treatment of rheumatism, arthritis, bone-muscle traumatic damage and skin diseases, as local or generalized

* E-mail: mrebelo@ua.pt

DOI: 10.1180/claymin.2010.045.2.229

---

[1] Empirical applications are those whose therapeutic effects were observed and experienced without any thorough scientific studies.

cataplasms. Also, clay minerals are used in cosmetic cleaning masks and in aesthetic clay-water baths to recover lipo-dystrophies and cellulitis. Pelotherapy (or mudtherapy) is the use of clay pastes (also called thermal muds or peloids) for internal or external therapeutic applications.

Thermal muds are hydrothermal pastes, produced by mixing clayey geomaterials with salty thermo-mineral waters in a process known as maturation; it is usually used for its stimulatory, anti-inflammatory and analgesic action. This therapeutic efficiency depends mainly on the mineralogical and chemical composition of the clay, as well as its technological properties (Ferrand & Yvon, 1991).

The main physicochemical properties shown by thermal muds are a large specific surface area, high cation exchange capacity, high specific heat and small rate of heat diffusivity (Carretero & Pozo, 2007; Legido *et al.*, 2007; Tateo & Summa, 2007). Other parameters influencing thermal mud efficiency, such as a large content of swelling-exchanging clay minerals and large clay fraction content, are also required as they are responsible for good water/heat retention and absorptive capacity. Good consistency and bio-adhesiveness, ease of handling, pleasant sensation when applied to the skin, cooling kinetics and exchange capacity through mud/skin interface, are a result of these properties and typical of a mature thermal mud (Veniale *et al.*, 2004, 2007).

In the present work, the suitability of clays for therapeutic and aesthetic purposes were assessed according to the following parameters: granulometry, mineralogy, chemistry and physicochemical properties. These parameters are responsible for the therapeutic properties of thermal muds with their application at thermal centres (Veniale *et al.*, 2004, 2007; Carretero & Pozo, 2007; Legido *et al.*, 2007; Tateo & Summa, 2007).

Over the past three years, our research has been aimed at gaining insight into the physicochemical and mineralogical properties of some Portuguese Mesozoic-Cenozoic clayey materials, some of which have had therapeutic outdoor applications in historical times (Rebelo *et al.*, 2005; Terroso *et al.*, 2006). Hence, our main goal was the selection of potential suitable materials for the formulation of thermal muds and promoting their application in Portuguese thermal centres. Taking into account that the studied materials may require initial separation of the silt-clay fraction (<63 μm) to allow application of clay paste without disturbing the treatment, this study focused on the silt-clay fraction.

MATERIALS AND METHODS

Materials

We have studied samples from selected smectite-bearing Portuguese Mesozoic-Cenozoic sedimentary formations (Oliveira *et al.*, 2002). Diverse geomaterials with empirical applications were collected from Jurassic to Miocene age deposits (Rebelo *et al.*, 2005) near thermal centres and beaches (Fig. 1).

Jurassic materials were collected near Vimeiro thermal centre and at Consolação beach. They include Dagorda grey marls (VM8), Abadia marly clays (VM9) and Consolação dark marly clays (CSB). Lower Cretaceous clayey materials were collected at Burgau beach and include green clays (BRG1, LUZ1 and PMOS1). Miocene materials were collected near Monfortinho thermal centre and Meco beach including: Sado Bassin clayey sandstones (GL10), Torre grey marls (MON7) and Penedo dark clays (PN11). Finally, bentonitic materials were collected near Nisa thermal centre and include alteration products of Benavila (BV4.2, VL1) and Pedrógão (MR1) Hercynian eruptive rocks. The location of these geological formations is shown in Fig. 1.

Methods

Wet sieving. Approximately 500 g of bulk sample was wet sieved with 1 litre of distilled water on a <63 μm sieve to separate silt-clay fraction (<63 μm) from sand-gravel fraction (>63 μm). After drying at 50–60°C, the silt-clay separated fractions were weighed and analysed. In samples VM8, VM9, MON7 and GL10, the cementing minerals were removed before wet sieving. The grain-size distribution was determined using an X-ray Sedigraph 5100 grain size analyser.

XRD analysis. Mineralogical analysis was carried out by X-ray diffraction (XRD) analysis with a Philips X-Pert diffractometer, using Cu-$K\alpha$ radiation. Random powder diffraction was used in the silt-clay fraction study (<63 μm). Air-dried and ethylene glycol solvated oriented aggregates of the clay fractions were prepared on glass slides. All oriented clay fractions were submitted to thermal treatment (300° and 500°C).

Semiquantitative estimates of the silt-clay fraction and clay mineral assemblages were achieved

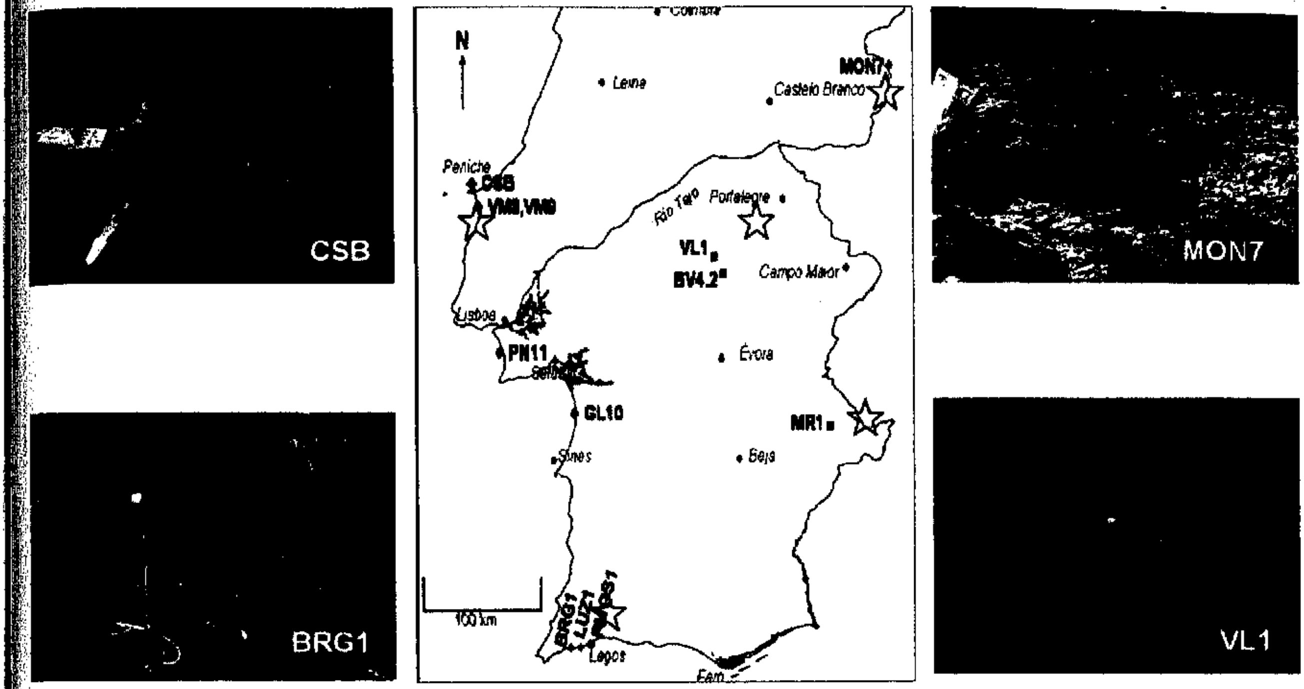

FIG. 1. Location of the samples studied and neighbouring thermal centres (stars). Adjacent images show some of the raw materials collected.

by measuring diagnostic peak areas which were determined by considering the full width at half maximum (FWHM), and then weighted by empirically estimated factors or reflection powers (Schultz, 1964; Biscaye, 1965; Galhano *et al.*, 1999; Oliveira *et al.*, 2002). The quartz content was estimated from the 4.26 Å reflection region, to avoid mica interference.

The peak area of the most intense reflection of phyllosilicates at a *d* value of 4.46 Å in non-oriented preparations was used to estimate the total proportion of clay minerals. Percentages of the different clay minerals were then obtained from the peak areas of diagnostic basal reflections of minerals in the diffractograms of the ethylene glycol solvated oriented aggregates. Given the uncertainties of the semiquantitative method, the results obtained should only be taken as rough estimates of mineral percentages. However, it was considered enough to define assemblages because presence/absence or dominant/subordinate relationships clearly allowed the establishment of distinct clay groups. The value of d_{060} was used to determine the octahedral character of all samples.

XRF and flame photometric analysis. Chemical compositions of major, minor and trace elements were determined by X-ray fluorescence (XRF) and flame-photometric methods, using a Philips

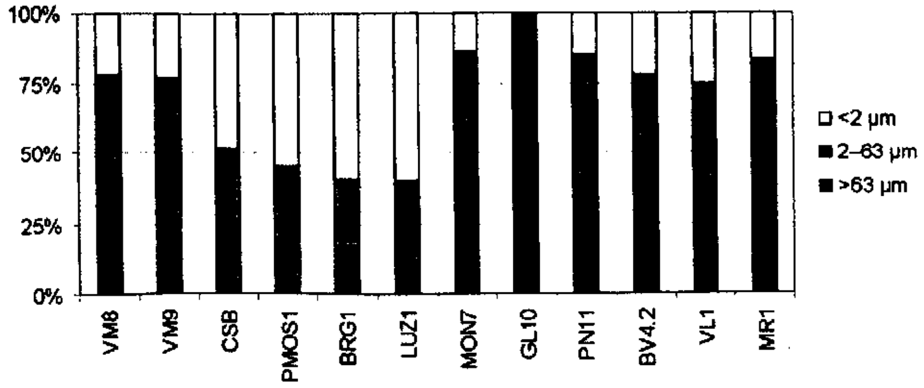

FIG. 2. Grain-size distribution assessed on silt-clay fractions.

PW1404 X-ray fluorescence spectrometer and a Coring 400 flame photometer (for Na and K).

EDS-SEM analysis. Chemical analyses were also carried out on the clay fractions with a scanning electron microscope (SEM) equipped with an energy dispersive X-ray spectrometer (EDS) which allowed image analysis of the surface of the clay minerals (Delgado *et al*., 1992).

The clay fraction (<2 μm) was separated by sedimentation according to Stokes' Law. 10 g of the silt-clay fraction of each sample, previously disaggregated with a porcelain mortar were added to a test tube with 1000 ml of distilled water. To assess surface morphological properties and chemical analysis of clay particles, a portion (±1 g) of the clay fraction (powder) was fixed on a carbon sticker and then covered with graphite film. Criteria for clay mineral morphology, proposed by Henning & Störr (1986), were used in the interpretation of the electron micrographs. EDS chemical analyses were carried out on the surface of the clay particles.

Physicochemical properties. Specific surface area was determined by BET using Micromeritics Instrument Corporation Gemini II 2370 equipment. Cation exchange capacity was determined by the ammonium acetate method and exchangeable cations by atomic absorption spectrophotometry using GBC 906 Scientific Equipment. The plasticity index was calculated from Atterberg limits (Portuguese norm NP 143-1969) and the Casagrande test. The abrasiveness index was determined using Einlehner AT 1000 equipment and the swelling index according to the LNEC E200-1967 norm (Portuguese version of ASTM D4829-95 standard test method for expansion index of soils). The specific heat was determined on dried samples by differential scanning calorimetry (Shimatzu DSC-50) and heat diffusiveness by heating the dried sample in a small Teflon container up to 60°C and measuring the decrease of temperature to 30°C at room temperature (cooling rate) with a Dual Thermometer LT Lutron TM-906A .

RESULTS

Grain-size analysis

In general, samples contain more than 50% of the silt-clay fraction, except for MON7, GL10, BV4.2 and MR1 (Fig. 2). The clay fraction content is greatest in CSB, PMOS1, BRG1 and LUZ1.

Mineralogical composition (<63 μm)

For the majority of samples, the phyllosilicate content is ~50%, always accompanied by some quartz (Table 1). Other detrital minerals, such as K-feldspar and plagioclase, are abundant, especially in samples VM8, VM9, LUZ1, MON7, PN11 and VL1. In fact, only CSB, PMOS1, BRG1, GL10 and BV4.2 have small quartz contents (BV4.2 is quartz free).

TABLE 1. Mineralogical composition of the clay samples (wt.%).

Sample	VM8	VM9	CSB	PMOS1	BRG1	LUZ1	MON7	GL10	PN11	BV4.2	VL1	MR1
Quartz	32	17	5	2	6	15	30	1	20	0	21	10
K-feldspars	8	9	0	0	1	1	4	3	2	1	5	10
Plagioclases	8	5	4	0	1	1	2	0	15	1	10	15
Kaolinite	20	5	5	0	5	0	10	65	5	0	3	0
Mica-illite	21	29	32	50	65	70	20	20	30	0	20	5
Palygorskite	0	0	0	0	0	0	20	0	0	20	0	0
Smectite	0	12	5	0	0	0	2	0	12	65	13	43
Chlorite	3	9	5	0	0	2	4	1	0	5	0	10
Calcite	0	9	30	42	12	0	0	1	6	5	16	5
Dolomite	2	0	8	0	0	0	0	0	0	0	0	0
Siderite	1	0	1	0	0	0	1	0	2	0	0	0
Iron oxides	4	5	4	6	10	11	5	4	4	0	3	2
Cristobalite	1	0	0	0	0	0	0	0	2	0	5	0
Anhydrite	0	0	1	0	0	0	2	0	0	0	4	0
Halite	0	0	0	0	0	0	0	5	2	0	0	0
Hornblende	0	0	0	0	0	0	0	0	0	3	0	0

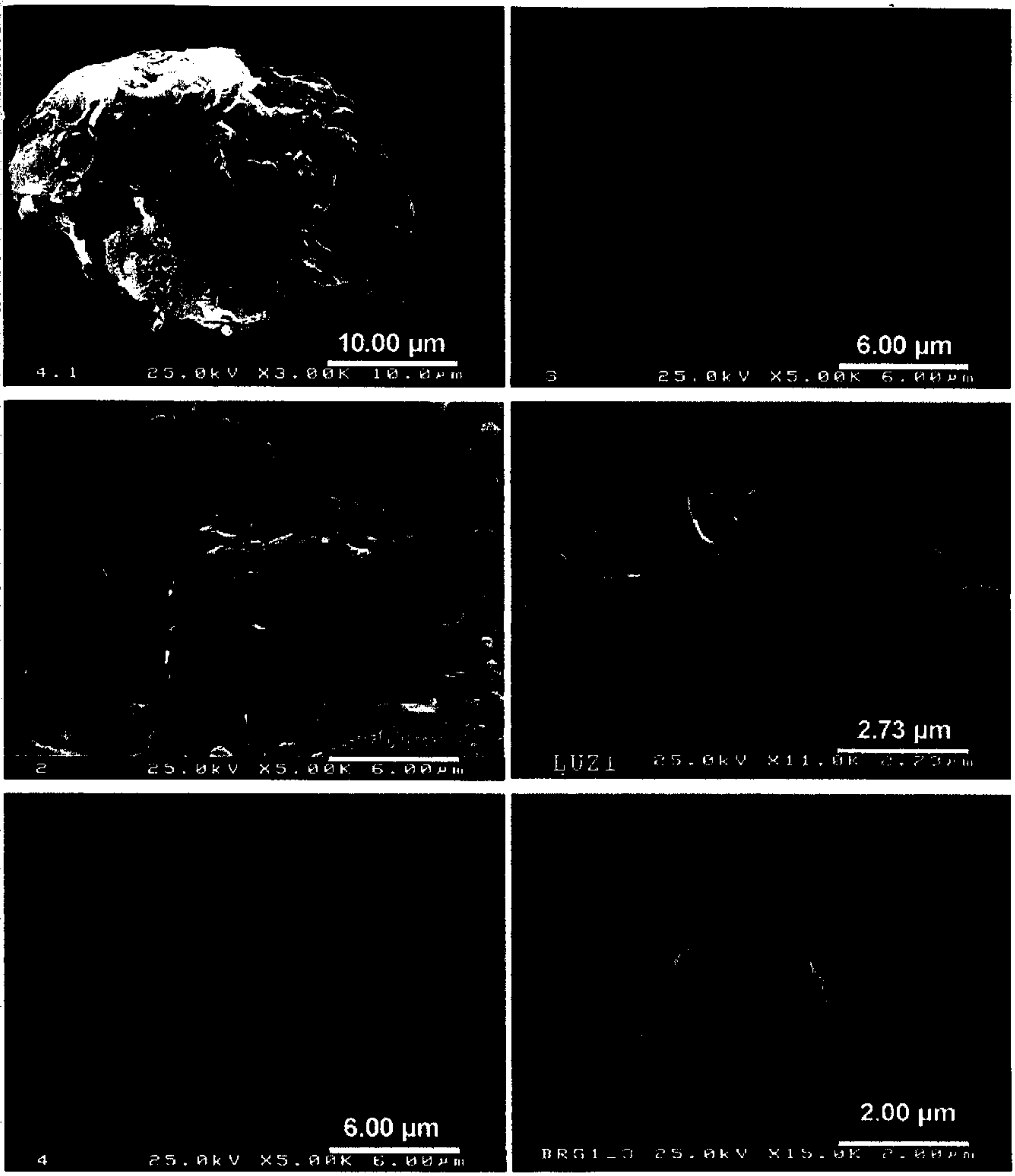

FIG. 3. Representative SEM images of clay particles. Images on the left correspond to particles in samples BV4.2, VL1 and MR1. Images on the right correspond to particles in samples CSB, LUZ1 and BRG1.

Carbonates, such as calcite and dolomite, are also present in all samples except for LUZ1 and MON7 (Table 1). Calcite is the most common carbonate, being abundant in CSB, PMOS1, BRG1 and VL1 while dolomite and siderite are present in a few samples. Fe oxides are present in all samples, especially BRG1 and LUZ1. Cristobalite, anhydrite and halite are present in trace amounts in a few samples. Hornblende was determined only in BV4.2.

TABLE 2. Major-element contents of the samples studied (wt.%). LOI = Loss on Ignition.

Sample	VM8	VM9	CSB	PMOS1	BRG1	LUZ1	MON7	GL10	PN11	BV4.2	VL1	MR1
SiO_2	67	56	35	28	45	58	64	43	63	50	57	58
Al_2O_3	15	17	14	10	17	18	15	30	14	12	12	21
Fe_2O_3	5	7	7	7	12	10	6	4	6	13	5	4
CaO	1	4	18	27	7	1	0	0	4	5	9	3
K_2O	3	4	4	4	6	6	3	2	3	0	2	2
MgO	1	2	3	2	1	1	3	1	2	6	2	3
TiO_2	1	1	1	0	1	1	1	0	1	0	1	0
Na_2O	1	1	0	0	1	0	1	3	1	0	1	1
LOI	6	8	18	22	10	5	7	17	6	14	11	8

The most common clay mineral is illite, usually accompanied by kaolinite and, in a few samples, smectite (Table 1). The exceptions are GL10, in which kaolinite is more common, and BV4.2 and MR1, in which smectite is the main clay mineral. Chlorite is also present in a few samples but is never >10%. Palygorskite is the less common clay mineral; it was observed on MON7 and BV4.2, never >20%. Therefore samples BRG1 and LUZ1 can be classified as illitic clays, GL10 is kaolinitic and BV4.2 is smectitic. Nevertheless illite is the most common clay mineral among the studied samples.

According to the d_{060} reflections, all samples were characterized mainly by dioctahedral clay minerals, the most common being illite-muscovite. In BV4.2, MR1, VL1 and VM9 the most abundant mineral is smectite. Trioctahedral/di-trioctahedral clay minerals were also determined in PN11 and MON7 (minor biotite and palygorskite).

SEM-EDS analysis

SEM images of clay particles showed two representative morphologies (Fig. 3). Samples with greater illite contents, such as BRG1 and LUZ1, are characterized by elongated and transparent platy particles with irregular contours (Fig. 3). EDS analysis showed an abundance of K, Fe and Ca, confirming the presence of illite.

In smectitic samples, such as BV4.2, MR1 and VL1, the surface of larger clay particles display a scaly arrangement, often with folded contours (Fig. 3). EDS analysis of these particles showed the presence of Ca and Mg. Na is a less common element observed in EDS spectra. It is common in illitic samples whereas in smectitic it was observed only in MR1.

The SEM studies confirmed the abundance of illite in the samples analysed. Isolated smectite particles and fibrous morphologies were not observed in samples MON7 and BV4.2. EDS

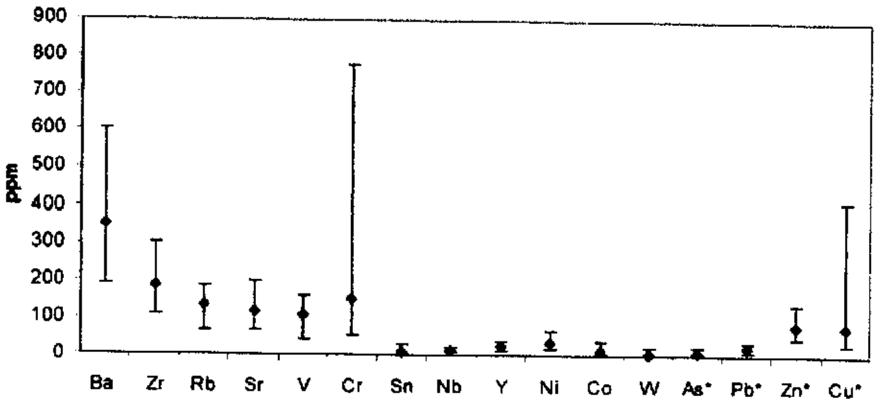

FIG. 4. Trace elements in the samples studied. Potentially toxic elements are marked by asterisk (*).

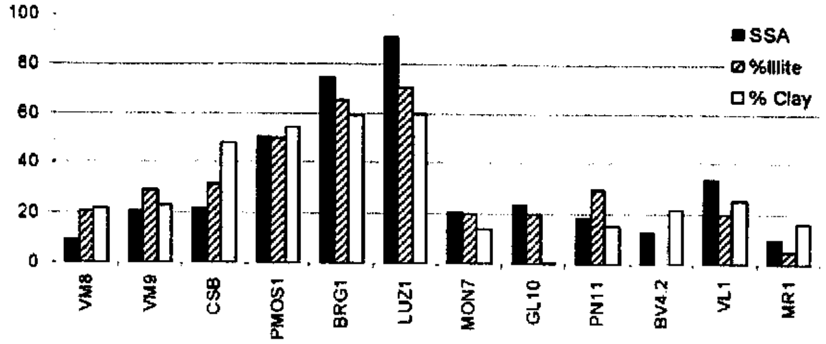

FIG. 5. Distribution of specific surface area in the samples studied.

analysis confirmed that the phyllosilicates analysed have large K, Mg, Ca and Fe contents. These EDS results, together with XRD d_{060} reflections, showed that some of these clay particles are dioctahedral smectites from the beidellite–montmorillonite series.

Chemical composition

Silica is the more abundant major oxide, except for sample PMOS1 which contains abundant carbonates (Table 2). The greatest SiO_2 contents were observed in VM8, MON7 and PN11, while Al_2O_3 and Fe_2O_3 are present in minor quantities. GL10 is the more aluminous and BV4.2, LUZ1 and BRG1 are the more Fe-rich samples. Ca, K and Mg are the less abundant major elements. Exceptions are observed in those samples rich in carbonates (CSB and PMOS1). Na and Ti are present in trace quantities, with GL10 having a greater Na content. Loss on ignition (LOI) is usually ~10%, but in CSB, PMOS1 and GL10 it reaches 20%.

Barium is the most abundant trace element, reaching 300 ppm on average. Sample BV4.2 has a greater Cr content (Fig. 4). Among the chemical elements which are potentially toxic and not allowed in cosmetic products, Zn and Cu are considered to be the main hazardous ones. They exhibit the greatest values compared with As and Pb. Apparently, these concentrations are not considered dangerous, although in sample PN11, Cu is abundant (553 ppm).

Physicochemical properties

Specific surface area. The majority of samples (Fig. 5) exhibit specific surface area (SSA) values of ~20 $m^2 g^{-1}$ (PMOS1, BRG1 and LUZ1 have greater values). There is a positive relation between SSA values and clay fraction content, mainly in samples which contain illite as the main clay mineral (Fig. 6).

Cation exchange capacity. The cation exchange capacity (CEC) of the samples investigated (Table 3) is <20 meq/100 g (VM9, MON7, BV4.2, VL1 and MR1 have greater values). The CEC values seem to be associated with the smectite content. The main exchangeable cation is Ca^{2+} except for PMOS1, BRG1, LUZ1 and GL10 in which the main exchangeable cation is Na^+ (see Table 3) and in BV4.2 and MON7 which have abundant exchangeable Mg^{2+} and Ca^{2+}.

Technological properties. The plasticity index varies generally between 10 and 20% (MON7 and MR1 showing greater values). Liquid limits (LL) are >50% in LUZ1, MON7, PN11, BV4.2, VL1 and

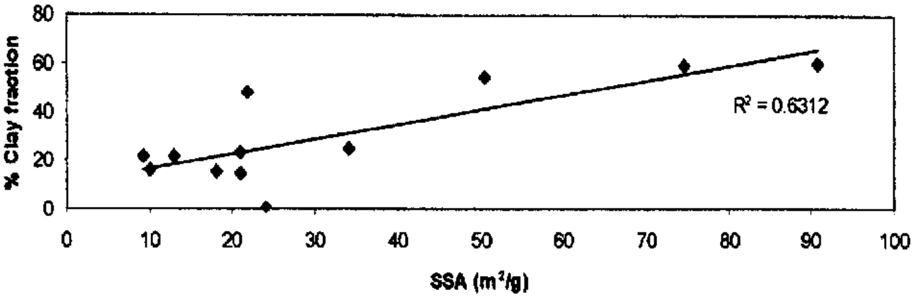

FIG. 6. Pearson's correlation between the clay fraction content and SSA values in the samples studied.

TABLE 3. Exchangeable cations and respective CEC values (cmol kg^{-1}). ΣCat = sum of exchangeable cations.

Sample	VM8	VM9	CSB	PMOS1	BRG1	LUZ1	MON7	GL10	PN11	BV4.2	VL1	MR1
Ca^{2+}	6	39	48	1	0	0	4	3	33	28	32	26
Mg^{2+}	1	4	0	1	2	2	4	14	2	27	6	10
Na^{+}	3	3	6	48	45	5	0	93	6	1	2	0
K^{+}	1	1	1	1	1	2	1	2	1	0	0	0
ΣCat	11	47	55	51	48	9	9	112	42	56	40	36
CEC	13	25	7	3	8	12	20	12	13	73	20	68

MR1, the last one showing LL >100%. Plastic limits are ~30%, being greater in those samples with higher LL values (Table 4). When projected onto a Casagrande Chart (Fig. 7), only three samples (BV4.2, MON7 and MR1) can be classified as high-plasticity clays.

The swelling index values are usually ~30% and only BV4.2 reaches 50%. The abrasiveness index (Table 4) is ~0.15 g m^{-2} in the majority of the samples, with CSB, PMOS1, BRG1 and GL10 being less abrasive.

Thermal properties. The samples usually cooled from 60 to 30°C within 15–30 min (Fig. 8). The smallest cooling rate was observed for BV4.2 (cooling achieved in 30 min) and the greatest rates were observed for PMOS1, BRG1 and LUZ1. Specific heat values varied significantly and occasionally exceeded 2 J/g°C. In sample BV4.2 the specific heat was almost 3 J/g°C.

DISCUSSION

Mineralogy and geochemistry

Most of the samples have small proportions of clay (Fig. 2) and only a few can be considered as clayey materials (PMOS1, BRG1, LUZ1). This scarcity of clay particles, related to the origin of the samples, influences some important technological properties, such as specific surface area, cation exchange capacity, consistency and abrasiveness. The Fe content of sample BV4.2 is related to the presence of an Fe-rich montmorillonite, which is typical of hydrothermal alteration of eruptive rocks (Weaver & Pollard, 1975) cropping out in the areas studied. This fact can also explain the greater than expected value for Cr (0.104% in the bulk sample). According to Weaver & Pollard (1975), Cr_2O_3 is present in some Fe-bearing dioctahedral montmorillonites/nontronites which are associated with altered basalts (Koster, 1960). Furthermore, this is a typical concentration for ultrabasic magmatic rocks (Carretero & Pozo, 2007). Before assessing Cr toxicity and bioavailability, it is important to determine its oxidation state (Cr^{4+} or Cr^{6+}) since this determines its toxicity. This will take place in further work.

The concentration of Cu is eight times the normal concentration of Cu in soils (Carretero & Pozo, 2007). This may be related to the weathering of sulphides. Although in sample PN11 pyrite and

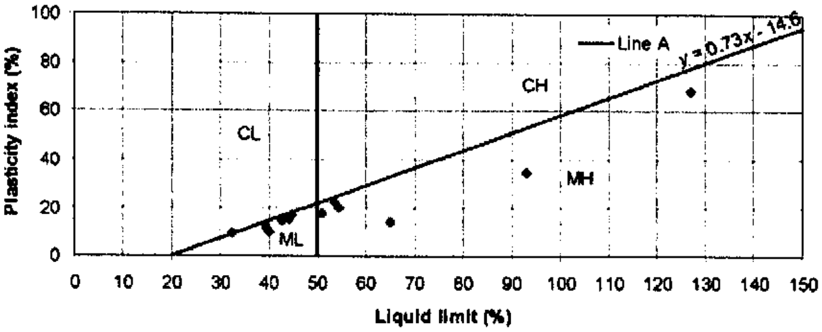

FIG. 7. Projection of plasticity indices and liquid limits in the Casagrande chart. Line A is an empirical boundary for classification of cohesive soils (Bain, 1971). CH, high-plasticity. clays; CL, low-plasticity clays; ML and MH, silt and organic soils of low and high plasticity

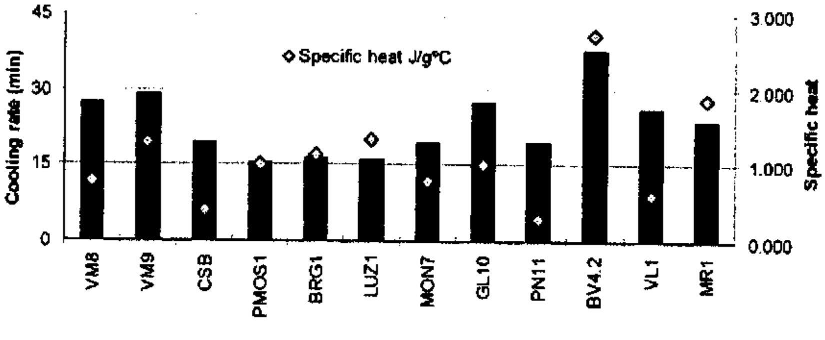

FIG. 8. Heat diffusiveness and specific heat values of the samples studied.

chalcopyrite were not detected, the surrounding rocks contain up to 8% of these minerals (Silva, 1999). Sample PN11 could be toxic for these applications and the bio-availability of Cu must be checked, especially considering that this sample is being used in empirical applications.

According to European directives, trace elements such as As, Se, Cd, Hg, Te, Tl and Pb are not allowed in cosmetic materials, including clays and peats for pelotherapy (European regulation n.85/391/CEE, 86/179/CEE and 86/199/CEE). In addition, Canada and United States F.D.A. (Food and Drug Administration) regulations also state that heavy metal concentrations in cosmetic products must be avoided if they exceed 10 ppm in the case of Pb, 3 ppm for As, Cd, Hg and 5 ppm for Sb.

From a geochemical standpoint the concentrations of Pb and As in the samples studied approximate to their abundances in Earth's upper crust (Li, 2000) as well as to those obtained in commercial muds and face masks made from material sourced from the Dead Sea (Abdel-Fattah & Pingitore, 2009). However, from a risk standpoint, only sample BV4.2 meets the US and Canada regulations regarding the abundances of As and Pb.

Physical and chemical properties

The specific surface area is typical of illitic clays (Carretero & Pozo, 2007) and is also related to the sizes of the clay fraction. This is the reason why samples such as BV4.2 and MR1, although having large smectite contents in the clay fractions, have small specific surface area values due to their small clay fraction content. The cation exchange capacity is also typical of illitic clays (Carretero & Pozo, 2007), although on the more carbonated samples (PMOS1, BRG1, LUZ1 and CSB) larger values were expected (Dohrmann, 2006). In these cases, CEC and exchangeable cation values are often inflated to a large extent, because carbonates are partially dissolved during the exchange experiments and interact with electrolyte-rich solutions.

The sum of exchanged cations is not equivalent to the cation exchange capacity (Table 3). After re-

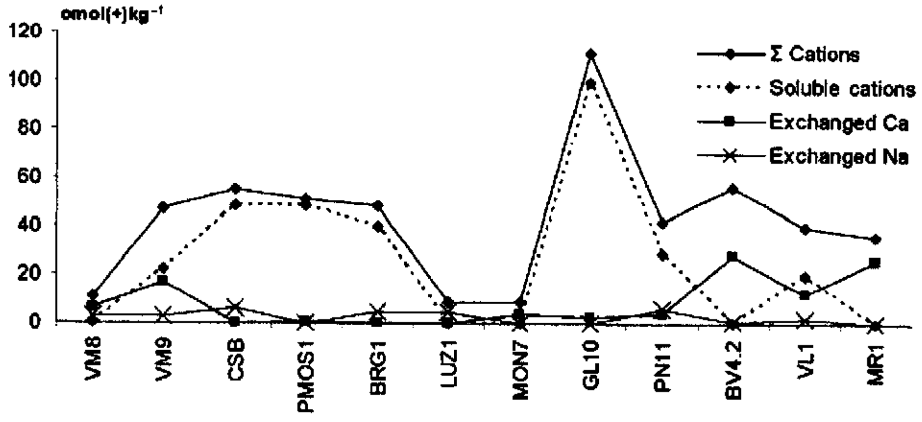

FIG. 9. Relationship between exchangeable cations and soluble cations (Extracted from *Health Canada Draft Guidance on Heavy Metal Impurities in Cosmetics* on www.hc-sc.gc.ca/cps-spc/legislation/consultation/_cosmet/metal-metaux-consul (07-08-2009).

TABLE 4. Technological properties of the samples studied.

Sample	VM8	VM9	CSB	PMOS1	BRG1	LUZ1	MON7	GL10	PN11	BV4.2	VL1	MR1
Atterberg limits												
Liquid limit %	32	43	39	45	44	51	93	40	54	65	54	127
Plastic limit %	23	28	28	28	29	33	58	30	32	51	35	59
Plasticity index %	9	14	11	17	15	18	35	10	22	14	20	68
Swelling %	12	29	16	– Not assessed –			25	9	21	51	30	45
Abrasiveness (g m^{-2})	0.17	0.19	0.06	0.05	0.07	0.15	0.11	0.04	0.22	0.14	0.25	0.08

distributing the number of soluble cations it was shown that only a few of the cations determined result from ion exchange. In fact, the majority of Ca^{2+} ions determined is in excess and results from carbonate dissolution (Fig. 9). In the particular case of Na^+, its excess can also result from the interaction with seawater in samples for which the location is near or inside tidal zones.

In sample GL10 the main exchangeable cation is Mg^{2+}, whereas in samples CSB and PN11 they are Na^+ and Ca^{2+}. Samples PMOS1 and BRG1 are poor in Na^+. Finally in samples VL1, BV4.2 and MR1, the main exchangeable cation is Ca^{2+} due to the presence of abundant smectite. In samples GL10, CSB, PN11, PMOS1, BRG1, VL1, BV4.2, MR1 and MON7 the sum of exchangeable cations is smaller than the CEC. According to Roth *et al.* (1969) and Zhuang & Yu (2002), positively charged coatings such as metal oxides may be adsorbed on clay particle surfaces and thus they may partly balance the negative layer charge. These positively charged coatings may be dissolved, liberating negative charges and increasing the CEC (Favre *et al.*, 2006).

The plasticity indices and Atterberg limits are small, even for illitic materials (only samples BV4.2, MON7 and MR1 have high plasticity), probably due to the large number of non-clay components. The same is also observed for swelling properties. In terms of water absorption, the smectite-rich BV4.2 and MR1 display maximum adsorption although the observed swelling is smaller than expected for smectite-rich materials. The quartz-rich samples exhibit larger values of abrasivity (Table 1). In sample BV4.2 which is quartz-free, the abrasivity observed is due to the presence of mafic minerals. Thermal properties are adequate in almost all samples because the common duration of a treatment by application of clays varies typically between 15 and 30 min. Only PMOS1, BRG1 and LUZ1 have cooling rates that could be considered inadequate. Specific heat values are also in accordance with those of typical therapeutic clays (Carretero & Pozo, 2007), although samples CSB and PN11 have specific heat values which are too small for these applications.

FUTURE WORK

The small phyllosilicate content is a remarkable characteristic of the samples examined. According to Veniale (2007), this disadvantage can be

TABLE 5. Overall physicochemical properties of the samples studied.

Surveyed parameters	Properties established
Composition and texture	Small amount of clay particles
	Abundant detrital minerals and carbonates
	Small amount of phyllosilicates
	Small smectite content
	Essential elements such as Si, Al, Ca and Fe are present
	Hazardous elements present at normal values
Absorption and exchange	Low specific surface and swelling capacity
	Small cation-exchange capacity
	Samples exchange mainly Ca^{2+}
Application and topical use	Good plastic properties
	Some abrasivity is expected
	Good heat retention capacity
	No fibrous morphologies
	Elongated particles and thin particles.
	Scarce smectite particles (montmorillonite)

improved by blending with a phyllosilicate-rich clayey material. Also, the physicochemical properties can be improved during maturation. Further research will establish the effect of the admixture of clayey materials with minero-medicinal water of different characteristics and phyllosilicate-rich clayey material.

On the other hand, the determination of rheological properties will allow the assessment of the efficiency of these clays for topical treatment, since this property suggests their suitability for treatment (Carretero & Pozo, 2007). Furthermore, other important parameters for evaluating the effectiveness of thermal mud applications on the body skin, such as bio-adhesiveness and adsorption capacity, need to be assessed. In order to address other important aspects referred to in the present work, the mobility of some potentially hazardous chemical elements such as Cr and Cu needs to be assessed by leaching and bio-availability tests (Tateo & Summa, 2007).

CONCLUSIONS

The samples studied here have a medium to small phylllosilicate content and contain a relatively small amount of swelling clay minerals with CEC. The clay fraction content is also small, and some abrasive minerals are present. The chemical composition varies considerably, but concentrations of hazardous elements present a limited risk. These compositional and textural characteristics affect some relevant parameters required for therapeutic use. In fact, the samples exhibit small specific surface areas and low cation exchange capacities. However, they still have good application potential, especially in applications which require thermal properties and consistency. A summary of the physicochemical properties obtained is depicted in Table 5. Based on their properties, for therapeutic/cosmetic purposes bentonitic materials are the most suitable for the formulation and warm application of both geotherapy and pelotherapy. Nonetheless, the remaining groups may also be suitable, especially for heat treatments.

REFERENCES

Abdel-Fattah A. & Pingitore N.E. Jr (2009) Low levels of toxic elements in Dead Sea black mud and mud-derived cosmetic products. *Environmental Geochemistry and Health*, **31**, 487–492.

Bain J.A. (1971) A plasticity chart as an aid to the identification and assessment of industrial clays. *Clay Minerals*, **9**, 1–17.

Biscaye E.P. (1965) Mineralogy and sedimentation of Recent deep sea clay in the Atlantic Ocean and adjacent seas and oceans. *Geological Society of America Bulletin*, **76**, 803–831.

Carretero M.I. (2002) Clay minerals and their beneficial effects upon human health. A review. *Applied Clay Science*, **21**, 155–163.

Carretero M.I. & Pozo M. (2007) *Mineralogia Aplicada*

– *salud y Medio Ambiente*. Thompson Editores (Spain).

Delgado R., Soriano M., Delgado G. & Gámiz E. (1992) *Study of the mineralogical components of pharmaceutical and cosmetic products using SEM*, **2.** EUREM 92, Granada, Spain.

Dohrmann R. (2006) Cation exchange capacity methodology I: An efficient model for the detection of incorrect cation exchange capacity and exchangeable cation results. *Applied Clay Science*, **34**, 31–37.

Favre F., Bogdal C., Gavillet S. & Stucki J.W. (2006) Changes in the CEC of a soil smectite-kaolinite clay fraction as induced by structural iron reduction and iron coatings dissolution. *Applied Clay Science*, **34**, 95–104.

Ferrand T. & Yvon J. (1991) Thermal properties of clay pastes for pelotherapy. *Applied Clay Science*, **6**, 21–38.

Galhano C., Rocha F. & Gomes C. (1999) Geostatistical analysis of the influence of textural, mineralogical and geochemical parameters on the geotechnical behaviour of the Argilas de Aveiro formation (Portugal). *Clay Minerals*, **34**, 109–116.

Henning K.-H & Störr M. (1986) Electron micrographs (TEM, SEM) of clays and clay minerals. *Schriftenreihe für Geologische Wissenschaften, Series in Geological Sciences*, **25**. Akademie-Verlag, Berlin.

Koster H.M. (1960) Nontronit and Picotit aus dem Basalt des Okberges bei Hundsangen, Westerwald. *Contributions to Mineralogy and Petrology*, **7**, 71–75.

Legido J.L., Medina C., Mourelle M.L., Carretero M.I. & Pozo M. (2007) Comparative study of the cooling rates of bentonite, sepiolite and common clays for their use in pelotherapy. *Applied Clay Science*, **36**, 148–160.

Li Y.-H. (2000) *A Compendium of Geochemistry*. Princeton: Princeton University Press, USA.

Oliveira A., Rocha F., Rodrigues A., Jouanneau J., Dias A., Weber O. & Gomes C. (2002) Clay minerals from the sedimentary cover from the Northwest Iberian shelf. *Progress in Oceanography*, **52**, 233–247.

Rebelo M., Gonçalves P., Silva E. & Rocha F. (2005) Studies on physical and chemical properties of some Portuguese Mesocenozoic clayey formations traditionally used as curative or healing materials. *Acta Geodynamica et Geomaterialia*, **2** (2), 151–155.

Roth C.B., Jackson M.L. & Syers J.K. (1969) Deferration effect on structural ferrous-ferric iron ration and CEC vermiculites and soils. *Clays and Clay Minerals*, **17**, 253–264.

Schultz L.G. (1964) Quantitative interpretation of mineralogical composition from X-ray and chemical data for the Pierre Shale. *United States Geological Survey Professional Paper*, 391-C.

Silva A.P. (1999) *Mineralogia e geoquímica das fracções finas do Miocénico da Península de Setúbal: litostratigrafia e reconstituiçoes paleoambientais*. MSc thesis, Universidade Aveiro. Portugal.

Tateo F. & Summa V. (2007) Element mobility in clays for healing use. *Applied Clay Science*, **36**, 64–76.

Terroso D., Rebelo M., Santos A., Rocha F., Ferreira da Silva E., Patinha C. & Forjaz V.H. (2006) Hydrothermal clays from fumarolic fields (São Miguel and Terceira islands, Azores, Portugal) and its possible application in pelotheraphy. *Abstracts Joint Meeting Clay Minerals Society/French Clay Group* (Oleron, France), p. 256.

Veniale F., Barberis E., Carcangiu G., Morandi N., Setti M., Tamanini M. & Tessier D. (2004) Formulation of muds for pelotherapy: effects of maturation by different mineral waters. *Applied Clay Science*, **25**, 135–148.

Veniale F., Bettero A., Jobstraibizer P.G. & Setti M. (2007) Thermal muds: perspectives of innovations. *Applied Clay Science*, **36**, 141–147.

Weaver C.E. & Pollard L.D. (1975) *The Chemistry of Clay Minerals*. Elsevier Scientific Publishing Company, Amsterdam, The Netherlands.

Zhuang J. & Yu G.-R. (2002) Effects of surface coatings on electrochemical properties and contaminant sorption of clay minerals. *Chemosphere*, **49**, 619–628.